

# Resilient sliding mode control for 2D CPSs under denial-of-service attacks

Lingling LI<sup>1</sup>, Rongni YANG<sup>2</sup>, Zhiguang FENG<sup>1</sup> & Ligang WU<sup>1,3\*</sup><sup>1</sup>College of Intelligent Systems Science and Engineering, Harbin Engineering University, Harbin 150001, China;<sup>2</sup>School of Control Science and Engineering, Shandong University, Jinan 250061, China;<sup>3</sup>School of Astronautics, Harbin Institute of Technology, Harbin 150001, China

Received 13 April 2023/Revised 4 July 2023/Accepted 3 October 2023/Published online 13 May 2024

**Abstract** This study addresses the resilient sliding mode control (SMC) problem for two-dimensional cyber-physical systems (2D CPSs) characterized by the Roesser model under denial-of-service attack (DoS-A), which can interfere with signal transmission over the communication network. First, the DoS-A model is established by introducing constraints on the DoS frequency and duration. Then, based on active or silent attack situations, the considered system is described as a switched mode. Furthermore, together with Lyapunov theory, the average dwell time technique is employed to deduce sufficient criteria that assure the existence of the desired sliding mode controller. Finally, verification examples are provided to show the validity of the established SMC scheme.

**Keywords** two-dimensional systems, cyber-physical systems, denial-of-service attack, resilient sliding mode control

## 1 Introduction

With the rapid expansion of computer and communication technology, cyber-physical systems (CPSs) have gradually become an intensified research field and have attracted considerable attention in the control community. CPSs refer to systems that tightly combine physical resources, computation technologies, and communication networks, i.e., the cyber realm and physical layer (PL). For the cyber realm of CPSs, the system model commonly covers computation models, automata, and formal language. The main purpose is to realize security and privacy. Moreover, the control plant in the PL of CPSs can be modeled as a differential/difference equation and a 2D state-space model, and the control objective is to achieve system stability, good tracking, and optimal performance. CPSs are currently employed in a variety of fields, including smart homes and buildings, intelligent transportation, aerospace systems, medical and healthcare systems, and electric power grids. However, despite the characteristics of CPSs bringing great advantages, there are still challenges that cannot be ignored either. In particular, malicious attacks on CPSs can damage not only the cyber realm but also the PL. Thus, tremendous efforts have been exerted to address the issues of CPSs, and excellent achievements have been published [1–9].

Generally, security in CPSs primarily involves resilience against or protection from malicious attacks, e.g., denial-of-service attack (DoS-A) and deception attacks. In contrast to deception attacks, prior knowledge of the system model is unnecessary for adversaries to perform DoS-A, which is more profitable with a higher success rate from the perspective of attackers. Notably, the basic question for DoS-A is how to establish a suitable mathematical model. Generally, according to different attack strategies, DoS-A is categorized into frequency- and duration-constrained (FDC) DoS-A and stochastic DoS-A, which follow a probabilistic packet drop model. Compared with stochastic DoS-A, FDC DoS-A constrains the attacker's action by limiting the DoS frequency and duration, and it is more general and reasonable with practical motivation. Recently, considerable attention has been focused on the cybersecurity problem of CPSs subject to DoS-A, and significant results have been obtained [10–18]. For instance, a general DoS-A model with limitations on the attack frequency and duration was established in [10]; meanwhile, the

\* Corresponding author (email: [ligangwu@hit.edu.cn](mailto:ligangwu@hit.edu.cn))

input-to-state stability of CPSs was analyzed. In [12], the resilient sliding mode control (SMC) scheme based on a defense mechanism for CPSs subject to sensor DoS-A was proposed using zero-sum game theory. In [15], the observer-based output feedback controller was designed for CPSs under periodic DoS-A.

Notably, all of the aforementioned studies focused on the CPSs expressed by one-dimensional systems (1DSs). Nevertheless, with the popularization of informatization and networking, the requirement for multivariable/data processing is increasing. In particular, two-dimensional systems (2DSs), as a typical multivariable system, have the capabilities of modeling some practical processes whose dynamic behavior is characterized via independent variables, such as water stream heating, thermal processes, and sheet-forming processes [19–21]. In comparison with those of 1DSs, the states of 2DSs evolve in two independent directions, which can be expressed by partial differential/difference equations with more complicated dynamics. Consequently, the existing 1DSs theory is no longer applicable to 2DSs [22]. These facts have increased attention to research on the dynamic analysis problem of 2DSs [22–31]. Despite the significant achievements in addressing the issues of stability analysis, control, filtering, and estimation in 2DSs, less research on the cybersecurity problem of 2D CPSs has been conducted. Recently, preliminary results on the security issue of 2D CPSs have been obtained [32–34]. In [32], the resilient state feedback controller design problem of 2D CPSs encountering DoS-A was considered. However, throughout the analysis process, the characteristics of data transmission under DoS-A have not been reflected. In [33], the secure filtering issue was addressed based on 2D shift-varying systems under deception attacks, which were depicted by random variables following the Bernoulli distribution. Notably, in contrast to deception attacks that demand the secret information of CPSs, DoS-A is more general in practice. Therefore, it is of theoretical and practical importance to further explore the resilient control issue of 2D CPSs encountering DoS-A.

Moreover, SMC, as an effective and robust control scheme, has stirred a noticeable research interest in both control theory and engineering applications in recent decades. The core feature of SMC is the establishment of a suitable control strategy to enforce the system trajectory to a prescribed sliding surface and to stay on it with the desired properties. In contrast to various robust control strategies, the SMC approach has notable advantages, such as rapidity, strong robustness, and good transient performance. Considering the superiority of the SMC approach, numerous representative results on SMC have been reported for 1DSs [35–39]. In addition, given the theoretical significance of 2DSs, the SMC problem of 2DSs has been explored in the past few years [40–43]. Nevertheless, the resilient SMC problem of 2D CPSs under DoS-A has remained unsolved mainly because of the complexity caused by the multiple dimensions and special dynamics of 2DSs. This motivates us to investigate the security control problem of 2D CPSs using the SMC approach.

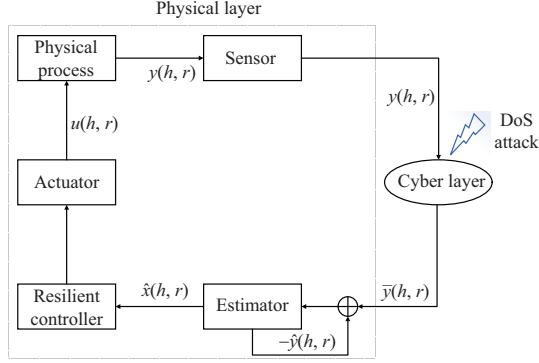
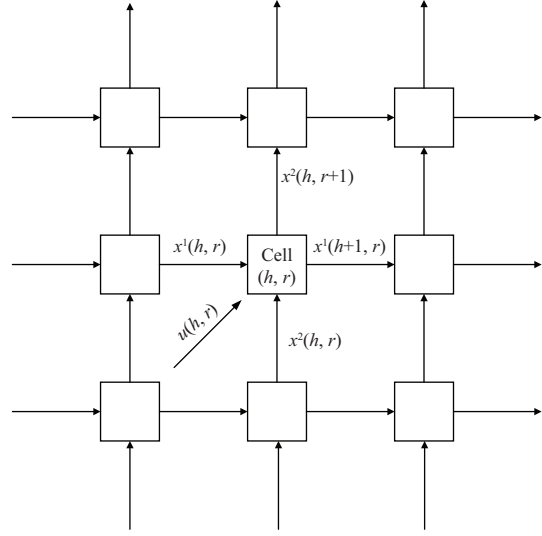
Thus, in this work, we address the security control issue of 2D CPSs using the SMC approach. The challenges that we are confronted with lie in three aspects: (1) How to establish the mathematical model of DoS-A given the bidirectional evolution of 2DSs and intermittent DoS-A? (2) How to construct a feasible sliding surface for 2DSs with horizontal and vertical components to guarantee the expected system performance? (3) How to design a suitable SMC law and analyze the reachability of the 2D sliding mode dynamic (SMD)? Therefore, the primary objective of this study is to overcome the aforementioned challenges. Furthermore, the main contributions of this study are listed as follows:

(i) The control plant in the PL of CPSs is expressed as a 2D Roesser model. Along with the intermittent DoS-A and bidirectional propagation of the 2D Roesser system, a proper mathematical model of DoS-A is proposed by introducing constraints on the frequency and duration of DoS.

(ii) Given that a DoS-A arises intermittently, the 2D CPSs under investigation are represented as a class of switched systems. With the help of the switched Lyapunov theory and the average dwell time (ADT) approach, sufficient criteria for the stability and  $H_\infty$  performance of the underlying systems are derived.

(iii) By constructing an appropriate sliding surface, the corresponding resilient SMC law is proposed to ensure the expected performance of 2D CPSs subject to DoS-A. This is our first attempt to address the resilient control issue of 2D CPSs using the SMC technique.

The remainder of this paper is organized as follows: Section 2 provides the system formulation and preliminaries, which include the 2D physical dynamic, DoS-A model, and construction of the estimator and sliding surface. Section 3 provides the theoretical result of the performance analysis and the design process of the resilient SMC scheme. Section 4 confirms the validity of the proposed SMC scheme using two examples. Finally, Section 5 presents the conclusion.


**Figure 1** (Color online) Diagram of CPSs.

**Figure 2** Dynamic evolution of the 2D Roesser model.

## 2 System description and preliminaries

A diagrammatic presentation of CPSs is shown in Figure 1, which incorporates the PL and cyber layer (CL). For the CL, only the sensor attack is considered. Figure 2 shows the evolution of the 2D Roesser model. Similar to the 1D state-space model, where the current state is evaluated using the previous state and input, the state vector components  $x^1(h+1, r)$  and  $x^2(h, r+1)$  of the 2D Roesser model are evaluated from the previous state and input. Notably, the information of the 2D Roesser systems propagates along the horizontal and vertical directions. Thus, the destruction of cell( $h, r$ ) influences both  $x^1(h+1, r)$  and  $x^2(h, r+1)$ . For convenience, cell( $h, r$ ) will be represented by cell( $l$ ) with  $l = h + r$ . Furthermore,  $l_1 = h_1 + r_1$  and  $l_2 = h_2 + r_2$ , and  $l_1 < l_2$  (i.e.,  $(h_1, r_1) < (h_2, r_2)$ ) means  $(h_2, r_2) \in \{(h, r) | h > h_1, r \geq r_1\} \cup \{(h, r) | h = h_1, r > r_1\}$ .

### 2.1 2D physical process

The control plant in the PL of CPSs is represented by the following 2D dynamical process:

$$\begin{cases} \begin{bmatrix} x^1(h+1, r) \\ x^2(h, r+1) \end{bmatrix} = Ax(h, r) + Bu(h, r) + D\omega(h, r), \\ y(h, r) = Cx(h, r), \end{cases} \quad (1)$$

where  $x(h, r) = [x^{1T}(h, r) \ x^{2T}(h, r)]^T$ ;  $x^1(h, r) \in \mathbb{R}^{i_h}$  and  $x^2(h, r) \in \mathbb{R}^{i_v}$  with  $h, r \in \mathbb{N}$  are the horizontal and vertical states, respectively;  $u(h, r) \in \mathbb{R}^{i_u}$  is the control input;  $\omega(h, r) \in \mathbb{R}^{i_\omega}$  is the external disturbance belonging to  $\ell_2\{[0, \infty), [0, \infty)\}$ ; and  $y(h, r) \in \mathbb{R}^{i_y}$  is the measured output.  $A = \begin{bmatrix} A_{11} & A_{12} \\ A_{21} & A_{22} \end{bmatrix}$ ,  $B = \begin{bmatrix} B_1 \\ B_2 \end{bmatrix}$ ,  $C = [C_1 \ C_2]$ , and  $D = \begin{bmatrix} D_1 \\ D_2 \end{bmatrix}$  are the system matrices, which are real known with appropriate dimensions. In addition, matrix  $B$  is assumed to be full-column rank. The boundary condition (BC) of system (1) is assigned as  $X_0 = \{x^1(0, r), x^2(h, 0) | h, r \in \mathbb{N}\}$  and satisfies the following condition:

$$\begin{cases} x^1(0, r) = \nu_r, \forall 0 \leq r \leq z_1, \quad x^2(h, 0) = \omega_h, \forall 0 \leq h \leq z_2, \\ x^1(0, r) = 0, \forall r > z_1, \quad x^2(h, 0) = 0, \forall h > z_2, \end{cases} \quad (2)$$

where  $\nu_0 = \omega_0$  for  $h = r = 0$ ,  $\nu_r$  and  $\omega_h$  are given vectors, and  $z_1$  and  $z_2$  are positive integer values.

### 2.2 Denial-of-service attacks

With regard to DoS-A, the objective of the attacker is to degrade the system performance by disrupting data transmission and reception on communication channels. In this study, we only consider the attack on

the measurement channel (i.e., sensor attack), which leads to missing state information. In addition, for cell( $h, r$ ), the emergence or absence of DoS-A depends on the time instant  $l$  with  $l = h + r$ . Furthermore,  $\{l_i\}_{i \in \mathbb{N}}$  denotes the moment of DoS off/on switching. Then,  $\Gamma_i \triangleq l_i \cup [l_i, l_i + \tau_i)$  denotes the  $i$ -th activated time interval of DoS-A with the length  $\tau_i \geq 0$ . If  $\tau_i = 0$ , then the  $i$ -th DoS-A is launched merely at instant  $l_i$ .  $\tau_i > 0$  indicates that data transmission is interrupted between cell( $l_i$ ) and cell( $l_i + \tau_i$ ).

For an interval  $(k, l)$  with  $k = h_0 + r_0$ ,  $l = h + r$ , and  $0 \leq k \leq l$ , two types of subintervals, i.e.,  $\mathcal{F}_1(k, l)$  and  $\mathcal{F}_2(k, l)$ , which denote active and silent attacks on the interval  $(k, l)$ , respectively, are defined and expressed as follows:

$$\mathcal{F}_1(k, l) = \bigcup_{i \in \mathbb{N}} \Gamma_i \cap (k, l), \quad \mathcal{F}_2(k, l) = (k, l) \setminus \mathcal{F}_1(k, l).$$

Notably, there is no overlap between  $\mathcal{F}_1(k, l)$  and  $\mathcal{F}_2(k, l)$ . Furthermore, the notations  $|\mathcal{F}_1(k, l)|$  and  $|\mathcal{F}_2(k, l)|$  represent the lengths of intervals  $\mathcal{F}_1(k, l)$  and  $\mathcal{F}_2(k, l)$ , respectively.

In practice, because of the defense mechanism and resource constraints, malicious DoS-A is not always persistent. Consequently, the following necessary assumptions on the DoS frequency and duration are made throughout this study.

**Assumption 1.** Within the interval  $(k, l)$ ,  $n(k, l)$  refers to the number of DoS-A. Then, given a constant  $T_D > 1$ , such that

$$n(k, l) \leq \frac{l - k}{T_D}. \quad (3)$$

**Assumption 2.** Within the interval  $(k, l)$ , in terms of the attack duration  $|\mathcal{F}_1(k, l)|$ , there exists a constant  $T_A > 1$ , such that

$$|\mathcal{F}_1(k, l)| \leq \frac{l - k}{T_A}. \quad (4)$$

**Remark 1.** Assumptions 1 and 2 depict the features of the DoS-A signals, which will be used subsequently. Notably, Assumption 1 resembles the expression of ADT, where  $n(k, l)$  refers to the number of DoS off/on transitions rather than the total switching times. In the interval  $(k, l)$ , the number of total switching can be expressed as  $\mathcal{N}(k, l) = n(k, l) + \bar{n}(k, l) \leq 2n(k, l) = \bar{\mathcal{N}}(k, l)$ , where  $\bar{n}(k, l)$  indicates the number of times the DoS switches on/off.  $T_D$  can be explained as the ADT of the coherent DoS off/on transition. If  $T_D = 1$ , DoS can occur at every instant, and stability will be lost. Assumption 2 indicates a requirement for the duration of DoS. The condition  $T_A > 1$  indicates that DoS-A cannot always be active.

### 2.3 Estimator design

Note that data transmission might be interrupted by malicious DoS-A. To compensate for the lost signals under DoS-A, an estimator is constructed as follows:

$$\begin{aligned} \begin{bmatrix} \hat{x}^1(h+1, r) \\ \hat{x}^2(h, r+1) \end{bmatrix} &= A\hat{x}(h, r) + Bu(h, r) + L_\theta e_y(h, r), \\ \hat{y}(h, r) &= C\hat{x}(h, r), \end{aligned} \quad (5)$$

where  $\hat{x}(h, r) = [\hat{x}^1(h, r), \hat{x}^2(h, r)]$  is the estimation of  $x(h, r)$ ,  $e_y(h, r) = \bar{y}(h, r) - \hat{y}(h, r)$ ,  $\bar{y}(h, r) \triangleq (1 - \delta(\theta, 1))y(h, r)$ , and  $\delta(\theta, 1)$  takes the value of 1 for  $\theta = 1$  and 0 otherwise. In addition,  $L_\theta = \begin{bmatrix} L_{1\theta} \\ L_{2\theta} \end{bmatrix}$  are the switching gains to be determined subsequently with  $\theta \in \{0, 1\}$ , where  $\theta = 1$  means that the DoS-A is activated and  $\theta = 0$  represents the normal circumstance.

### 2.4 Sliding surface design

The key issue in designing an SMC scheme is to establish a sliding surface and design a control signal. In this study, the following sliding surface function is constructed:

$$s(l) = s(h, r) = \begin{bmatrix} s^1(h, r) \\ s^2(h, r) \end{bmatrix} = G_\theta \hat{x}(h, r) - G_\theta (A + BK_\theta) \begin{bmatrix} \hat{x}^1(h-1, r) \\ \hat{x}^2(h, r-1) \end{bmatrix}, \quad (6)$$

where  $s^1(h, r)$  and  $s^2(h, r)$  are the horizontal and vertical subsiding surfaces, respectively, with  $l = h + r$ .  $G_\theta = [G_{1\theta} \ G_{2\theta}]$  are known matrices that satisfy the condition that  $G_\theta B$  is nonsingular.  $K_\theta = [K_{1\theta} \ K_{2\theta}]$  will be designed subsequently.

Furthermore, given the particularity of 2DS state recursion,  $s(l + 1)$  can be expressed as follows:

$$s(l + 1) = \begin{bmatrix} s^1(h + 1, r) \\ s^2(h, r + 1) \end{bmatrix} = G_\theta \begin{bmatrix} \hat{x}^1(h + 1, r) \\ \hat{x}^2(h, r + 1) \end{bmatrix} - G_\theta(A + BK_\theta) \begin{bmatrix} \hat{x}^1(h, r) \\ \hat{x}^2(h, r) \end{bmatrix}, \quad (7)$$

which satisfies  $s(l + 1) = s(l) = 0$ . Then, we obtain the following equivalent control law:

$$u_{eq}(h, r) = K_\theta \hat{x}(h, r) - (G_\theta B)^{-1} G_\theta L_\theta e_y(h, r). \quad (8)$$

Defining  $e(h, r) = x(h, r) - \hat{x}(h, r)$ , we obtain the following estimate error dynamic:

$$\begin{bmatrix} e^1(h + 1, r) \\ e^2(h, r + 1) \end{bmatrix} = A e(h, r) - L_\theta e_y(h, r) + D \omega(h, r). \quad (9)$$

Next, let  $\xi^1(h, r) = [\hat{x}^1(h, r)]$ ,  $\xi^2(h, r) = [\hat{x}^2(h, r)]$ . The combination of (5), (8), and (9) yields

$$\begin{aligned} \bar{\xi}(h, r) &= \tilde{A}_\theta \xi(h, r) + \tilde{D} \omega(h, r), \\ y(h, r) &= \tilde{C} \xi(h, r), \end{aligned} \quad (10)$$

where  $\bar{\xi}(h, r) = [\xi^1(h, r)]$ ,  $\xi(h, r) = [\xi^1(h, r) \ \xi^2(h, r)]$ ,  $\tilde{A}_\theta = \Xi A_\theta \Xi^T$ ,  $\tilde{D} = \Xi \bar{D}$ ,  $\tilde{C} = \bar{C} \Xi^T$ ,  $\bar{G}_\theta = (G_\theta B)^{-1} G_\theta$ ,  $\bar{D} = [0 \ D]^T$ ,  $\bar{C} = [C \ C]$ , and

$$A_0 = \begin{bmatrix} A + BK_0 & L_0 C - B \bar{G}_0 L_0 C \\ 0 & A - L_0 C \end{bmatrix}, \quad A_1 = \begin{bmatrix} A + BK_1 - L_1 C + B \bar{G}_1 L_1 C & 0 \\ L_1 C & A \end{bmatrix}, \quad \Xi = \begin{bmatrix} I & 0 & 0 & 0 \\ 0 & 0 & I & 0 \\ 0 & I & 0 & 0 \\ 0 & 0 & 0 & I \end{bmatrix}.$$

**Remark 2.** Notably, the SMD in (10) is described as a type of switched system based on the actual DoS-A situations. In contrast to the traditional 2D switched system that involves finite subsystems and a switching law, the system in (10) is depicted as a type of system consisting of stable (no attacks) and unstable (attack occurrence) modes. The ADT technique is commonly applied to address the related issues of switched systems. Similar to the analysis of ADT, in our study, the DoS-A frequency (Assumption 1) is adopted to discuss the SMC issue of 2D Roesser systems under DoS-A.

This study devises a resilient SMC scheme such that the SMD in (10) is exponentially stable (ES) with an  $H_\infty$  disturbance attenuation level. Furthermore, the following definitions of the main results are provided.

**Definition 1.** The SMD in (10) with  $\omega(h, r) \equiv 0$  is considered ES if the constants  $\eta > 0$  and  $0 < \rho < 1$  exist, such that

$$\sum_{h+r=\Pi} \|\xi(h, r)\|^2 \leq \eta \rho^{\Pi-l_0} \sum_{h+r=l_0} \|\xi(h, r)\|^2. \quad (11)$$

**Definition 2.** Given a scalar  $\vartheta > 0$ , the SMD in (10) under zero BC is considered ES with an  $H_\infty$  disturbance attenuation performance (DAP)  $\vartheta$ . If Eq. (11) and the following conditions hold:

$$\sum_{h=0}^{\infty} \sum_{r=0}^{\infty} \|y(h, r)\|^2 \leq \vartheta^2 \sum_{h=0}^{\infty} \sum_{r=0}^{\infty} \|\omega(h, r)\|^2. \quad (12)$$

**Remark 3.**  $H_\infty$  norm is a widely known performance index that indicates the robustness of an uncertain system. Robustness, as a pre-event concept, represents the capability of a system to resist disturbances or uncertain parameters. Generally, robust control is used to maintain the performance of the control

system under internal/external disturbances. In contrast to robustness, resilience, as a post-event concept, refers to the self-recovery capability of a system after adversarial events. Furthermore, the resilient control emphasizes the capability to maintain the performance of the control system and restore normal operation under unexpected attacks. Accordingly, to achieve self-recovery of the system under malicious attack, the design method of a resilient control scheme needs to be explored.

### 3 Main results

In this section, a resilient SMC scheme is proposed by combining the Lyapunov theory of switched systems and the linear matrix inequality (LMI) technique.

#### 3.1 Stability and $H_\infty$ performance of sliding mode dynamic

This subsection mainly focuses on the analysis of the stability and  $H_\infty$  performance of the SMD in (10). Sufficient criteria will be established to guarantee that the SMD is ES with an  $H_\infty$  attenuation performance  $\vartheta$ . To begin with, the following corollary is given, which is necessary for the subsequent main result.

**Corollary 1.** Consider the 2D dynamic process in (1) under DoS-A satisfying Assumptions 1 and 2 with the scalars  $0 < \varepsilon < 1$  and  $\alpha, \beta, \mu > 1$ . If the positive definite matrix  $P_\theta = \text{diag}\{P_\theta^1, P_\theta^2\}$  exists, such that

$$\begin{bmatrix} -\alpha P_1 & \tilde{A}_1^T P_1 \\ * & -P_1 \end{bmatrix} < 0, \quad \begin{bmatrix} -\frac{1}{\beta} P_0 & \tilde{A}_0^T P_0 \\ * & -P_0 \end{bmatrix} < 0, \quad (13)$$

$$P_\theta \leq \mu P_\delta, \quad \theta, \delta \in \{0, 1\}, \quad \theta \neq \delta, \quad (14)$$

$$\frac{\ln(\mu)}{\ln(\varepsilon) + \ln(\beta)} < \frac{T_D}{3}, \quad \frac{\ln(\alpha) + \ln(\beta)}{\ln(\varepsilon) + \ln(\beta)} < \frac{T_A}{3}, \quad \ln(\varepsilon) + \ln(\beta) > 0. \quad (15)$$

Then, the SMD in (10) with  $\omega = 0$  is ES.

*Proof.* First, construct the following Lyapunov function:

$$\begin{aligned} V_{\alpha(l)}(\xi(h, r)) &= V_{\alpha(l)}^1(\xi^1(h, r)) + V_{\alpha(l)}^2(\xi^2(h, r)) = \xi^T(h, r) P_{\alpha(l)} \xi(h, r), \\ V_{\alpha(l)}^1(\xi^1(h, r)) &= \xi^{1T}(h, r) P_{\alpha(l)}^1 \xi^1(h, r), \quad V_{\alpha(l)}^2(\xi^2(h, r)) = \xi^{2T}(h, r) P_{\alpha(l)}^2 \xi^2(h, r), \end{aligned} \quad (16)$$

where  $\alpha(l) = \theta \in \{0, 1\}$  and  $l = h + r$ . Then, by combining the SMD in (10) with  $\omega(h, r) = 0$ , we obtain the following expression:

$$\Delta V_{\alpha(l)}(\xi(h, r)) = V_{\alpha(l)}(\bar{\xi}(h, r)) - V_{\alpha(l)}(\xi(h, r)) = \bar{\xi}^T(h, r) P_{\alpha(l)} \bar{\xi}(h, r) - \xi^T(h, r) P_{\alpha(l)} \xi(h, r),$$

which indicates that

$$(1) \text{ for } \theta = 1 \text{ and } \omega(h, r) = 0, \quad \Delta V_{\alpha(l)}(\xi(h, r)) = \xi^T(h, r) [\tilde{A}_1^T P_1 \tilde{A}_1 - P_1] \xi(h, r);$$

$$(2) \text{ for } \theta = 0 \text{ and } \omega(h, r) = 0, \quad \Delta V_{\alpha(l)}(\xi(h, r)) = \xi^T(h, r) [\tilde{A}_0^T P_0 \tilde{A}_0 - P_0] \xi(h, r).$$

Furthermore, based on situations in which the DoS-A is successful or not, the following cases will be discussed.

(1) The system suffers from persistent DoS-A and evolves possibly unstable dynamics ( $l \in \mathcal{F}_1(k, l)$ ,  $\alpha(l) = \theta = 1$ ). Then, we derive  $\Delta V_{\alpha(l)}(\xi(h, r)) < (\alpha - 1) \xi^T(h, r) P_1 \xi(h, r)$  with  $\alpha > 1$ . Simultaneously, the following inequality holds:

$$\tilde{A}_1^T P_1 \tilde{A}_1 - P_1 < (\alpha - 1) P_1. \quad (17)$$

(2) The system operates normally without any attack, and its stability is well established ( $l \in \mathcal{F}_2(k, l)$ ,  $\alpha(l) = \theta = 0$ ). Thus, for  $\beta > 1$ , we derive  $\Delta V_{\alpha(l)}(\xi(h, r)) < (\frac{1}{\beta} - 1) \xi^T(h, r) P_0 \xi(h, r)$ , which can be written as follows:

$$\tilde{A}_0^T P_0 \tilde{A}_0 - P_0 < \left(\frac{1}{\beta} - 1\right) P_0. \quad (18)$$

(3) The system switches between situations (1) and (2) ( $l \in \mathcal{F}_1(k, l)$  or  $l \in \mathcal{F}_2(k, l)$ ), under which Eqs. (17) and (18) hold simultaneously. Furthermore, condition (13) can be inferred from (17) and (18) with the Schur complement. For the entire interval  $(0, l) = \bigcup_{i \in \mathbb{N}} [l_i, l_{i+1}) \cup [0, l_1]$ , let

$$\gamma = \begin{cases} \alpha - 1, & l \in \mathcal{F}_1(0, l), \\ \frac{1}{\beta} - 1, & l \in \mathcal{F}_2(0, l). \end{cases}$$

Then, according to (17) and (18), we derive  $\tilde{A}_\theta^T P_\theta \tilde{A}_\theta - P_\theta < \gamma P_\theta$  and

$$\Delta V_{\alpha(l)}(\xi(h, r)) < \gamma \xi^T(h, r) P_\theta \xi(h, r). \tag{19}$$

It follows from (19) that  $V_{\alpha(l)}(\tilde{\xi}(h, r)) < \bar{\gamma} V_{\alpha(l)}(\xi(h, r))$  with  $\bar{\gamma} = 1 + \gamma$ . Then, we derive

$$V_{\alpha(l)}^1(\xi^1(h+1, r)) + V_{\alpha(l)}^2(\xi^2(h, r+1)) < \bar{\gamma} [V_{\alpha(l)}^1(\xi^1(h, r)) + V_{\alpha(l)}^2(\xi^2(h, r))]. \tag{20}$$

From (2), it is inferred from (20) that, for the interval  $[l_i, l_{i+1})$ ,

$$\sum_{h+r=l} V_{\alpha(l)}(\xi(h, r)) < \bar{\gamma} \sum_{h+r=l-1} V_{\alpha(l)}(\xi(h, r)) < \bar{\gamma}^{l-l_i} \sum_{h+r=l_i} V_{\alpha(l_i)}(\xi(h, r)).$$

Recalling condition (14) in Corollary 1 and assuming  $\alpha(l_{i-1}) = \delta = \{0, 1\} \setminus \theta$ , we obtain the following inequality:

$$\begin{aligned} \sum_{h+r=l} V_{\alpha(l)}(\xi(h, r)) &< \bar{\gamma}^{l-l_i} \sum_{h+r=l_i} V_{\alpha(l_i)}(\xi(h, r)) < \mu \bar{\gamma}^{l-l_i} \sum_{h+r=l_i} V_{\alpha(l_{i-1})}(\xi(h, r)) \\ &< \mu^{\mathcal{N}(0, l)} \alpha^{|\mathcal{F}_1(0, l)|} \beta^{-|\mathcal{F}_2(0, l)|} \sum_{h+r=0} V_{\alpha(0)}(\xi(h, r)), \end{aligned}$$

where  $\mathcal{N}(0, l) = n(0, l) + \bar{n}(0, l)$  denotes the total number of systems switching between attack and normal modes. Then, the following inequality can be obtained:

$$\sum_{h+r=l} V_{\alpha(l)}(\xi(h, r)) < \mu^{\bar{\mathcal{N}}(0, l)} \alpha^{|\mathcal{F}_1(0, l)|} \beta^{-|\mathcal{F}_2(0, l)|} V_{\alpha(0)}(\xi(0, 0)),$$

where  $\bar{\mathcal{N}}(0, l) = 2n(0, l)$ . Recalling (3) and (4) in Assumptions 1 and 2, we obtain

$$\sum_{h+r=l} V_{\alpha(l)}(\xi(h, r)) \leq e^{\frac{2l}{T_D} \ln(\mu)} e^{\frac{l}{T_A} \ln(\alpha)} e^{-(l - \frac{l}{T_A}) \ln(\beta)} V_{\alpha(0)}(\xi(0, 0)). \tag{21}$$

In addition, it follows from (16) that  $a > 0$  and  $b > 0$  satisfy

$$V_{\alpha(l)}(\xi(h, r)) \geq a \|\xi(h, r)\|^2, \tag{22}$$

$$V_{\alpha(0)}(\xi(0, 0)) \leq b \|\xi(0, 0)\|^2, \tag{23}$$

where  $a = \min\{\lambda_{\min}(P_\theta), \theta \in \{0, 1\}\}$  and  $b = \max\{\lambda_{\max}(P_\theta), \theta \in \{0, 1\}\}$ . By combining (21), (22), and (23), we obtain  $\sum_{h+r=l} \|\xi(h, r)\|^2 \leq \frac{b}{a} e^{f(l)} \|\xi(0, 0)\|^2$  with  $f(l) = l(\frac{2}{T_D} \ln(\mu) + \frac{1}{T_A} \ln(\alpha) - (1 - \frac{1}{T_A}) \ln(\beta))$ . Then, based on condition (15), we derive  $f(l) < l \ln(\varepsilon)$  and  $\sum_{h+r=l} \|\xi(h, r)\|^2 \leq \frac{b}{a} (e^{\ln(\varepsilon)})^l \|\xi(0, 0)\|^2$  with  $0 < e^{\ln(\varepsilon)} < 1$  and  $\frac{b}{a} > 0$ , which indicate that Eq. (11) holds. Therefore, the SMD in (10) is ES, which completes the proof.

Subsequently, the theorem on exponential stability with an  $H_\infty$  DAP  $\vartheta$  for the SMD in (10) is established.

**Theorem 1.** Consider the 2D dynamic process in (1) under DoS-A satisfying Assumptions 1 and 2 with the scalars  $0 < \varepsilon < 1$ ,  $\vartheta > 0$ , and  $\alpha, \beta, \mu > 1$ . If the positive definite matrix  $P_\theta = \text{diag}\{P_\theta^1, P_\theta^2\}$  exists, such that the following inequalities:

$$\Phi_0 \triangleq [\Phi_0(h, r)]^{4 \times 4} < 0, \tag{24}$$

$$\Phi_1 \triangleq [\Phi_1(h, r)]^{4 \times 4} < 0, \tag{25}$$

hold with (14) and (15), where

$$\begin{aligned} \Phi_0(1, 1) &= -\frac{1}{\beta}P_0, \quad \Phi_0(1, 3) = \tilde{A}_0^T P_0, \quad \Phi_0(1, 4) = \tilde{C}^T, \quad \Phi_0(2, 2) = -\vartheta^2 I, \quad \Phi_0(2, 3) = \tilde{D}^T P_0, \\ \Phi_0(3, 3) &= -P_0, \quad \Phi_0(4, 4) = -I, \quad \Phi_1(1, 1) = -\alpha P_1, \quad \Phi_1(1, 3) = \tilde{A}_1^T P_1, \quad \Phi_1(1, 4) = \tilde{C}^T, \\ \Phi_1(2, 2) &= -\vartheta^2 I, \quad \Phi_1(2, 3) = \tilde{D}^T P_1, \quad \Phi_1(3, 3) = -P_1, \quad \Phi_1(4, 4) = -I. \end{aligned}$$

Then, the SMD in (10) is ES with an  $H_\infty$  DAP  $\vartheta$ .

*Proof.* With the Schur complement lemma, it follows from (24) and (25) that condition (13) holds. Consequently, the exponential stability of the SMD in (10) is assured. Next, we mainly focus on the  $H_\infty$  DAP for the considered system in (10) under zero BC. Let

$$\mathcal{J}_\theta = \Delta V_{\alpha(l)}(\xi(h, r)) + \mathcal{D}(h, r), \tag{26}$$

where  $\Delta V_{\alpha(l)}(\xi(h, r))$  is defined in the proof of Corollary 1 and  $\mathcal{D}(h, r) = y^T(h, r)y(h, r) - \vartheta^2 \omega^T(h, r)\omega(h, r)$ . By combining (10) and (24)–(26), we derive  $\mathcal{J}_\theta < \gamma V_{\alpha(l)}(\xi(h, r))$  with

$$\gamma = \begin{cases} \alpha - 1, & l \in \mathcal{F}_1(0, l), \\ \frac{1}{\beta} - 1, & l \in \mathcal{F}_2(0, l). \end{cases}$$

Then, letting  $\bar{\gamma} = 1 + \gamma$ , we obtain

$$V_{\alpha(l)}(\bar{\xi}(h, r)) < \bar{\gamma} V_{\alpha(l)}(\xi(h, r)) - \mathcal{D}(h, r). \tag{27}$$

From (27), we obtain

$$V_{\alpha(l)}^1(\xi^1(h + 1, r)) + V_{\alpha(l)}^2(\xi^2(h, r + 1)) < \bar{\gamma}[V_{\alpha(l)}^1(\xi^1(h, r)) + V_{\alpha(l)}^2(\xi^2(h, r))] - \mathcal{D}(h, r).$$

Furthermore, by applying the iteration technique, we derive

$$\sum_{h+r=l} V_{\alpha(l)}(\xi(h, r)) < \bar{\gamma}^{l-l_i} \sum_{h+r=l_i} V_{\alpha(l_i)}(\xi(h, r)) - \sum_{s=l_i}^{l-1} \sum_{h+r=s} \bar{\gamma}^{l-s-1} \mathcal{D}(h, r).$$

By selecting  $\alpha(l_{i-1}) = \delta = \{0, 1\} \setminus \theta$  and considering condition (14), we derive  $V_{\alpha(l_i)}(\xi(h, r)) < \mu V_{\alpha(l_{i-1})}(\xi(h, r))$  and

$$\begin{aligned} \sum_{h+r=l} V_{\alpha(l)}(\xi(h, r)) &< \mu \bar{\gamma}^{l-l_i} \sum_{h+r=l_i} V_{\alpha(l_{i-1})}(\xi(h, r)) - \sum_{s=l_i}^{l-1} \sum_{h+r=s} \bar{\gamma}^{l-s-1} \mathcal{D}(h, r) \\ &< \mu^{\mathcal{N}(0, l)} \alpha^{|\mathcal{F}_1(0, l)|} \beta^{-|\mathcal{F}_2(0, l)|} \sum_{h+r=0} V_{\alpha(0)}(\xi(h, r)) \\ &\quad - \sum_{s=0}^{l-1} \sum_{h+r=s} \mu^{\mathcal{N}(s, l)} \alpha^{|\mathcal{F}_1(s, l-1)|} \beta^{-|\mathcal{F}_2(s, l-1)|} \mathcal{D}(h, r). \end{aligned}$$

Then, the following inequality can be obtained under zero BC:

$$\begin{aligned} &\sum_{s=0}^{l-1} \sum_{h+r=s} \mu^{\mathcal{N}(s, l)} \alpha^{|\mathcal{F}_1(s, l-1)|} \beta^{-|\mathcal{F}_2(s, l-1)|} y^T(h, r)y(h, r) \\ &< \sum_{s=0}^{l-1} \sum_{h+r=s} \mu^{\mathcal{N}(s, l)} \alpha^{|\mathcal{F}_1(s, l-1)|} \beta^{-|\mathcal{F}_2(s, l-1)|} \vartheta^2 \omega^T(h, r)\omega(h, r). \end{aligned} \tag{28}$$

Multiplying both sides of (28) by  $\mu^{-\mathcal{N}(l-1, l)}$  yields

$$\sum_{s=0}^{l-1} \sum_{h+r=s} \mu^{\mathcal{N}(s, l-1)} \alpha^{|\mathcal{F}_1(s, l-1)|} \beta^{-|\mathcal{F}_2(s, l-1)|} y^T(h, r)y(h, r)$$

$$< \sum_{s=0}^{l-1} \sum_{h+r=s} \mu^{\mathcal{N}(s,l-1)} \alpha^{|\mathcal{F}_1(s,l-1)|} \beta^{-|\mathcal{F}_2(s,l-1)|} \vartheta^2 \omega^T(h,r) \omega(h,r).$$

From (15) with  $\mathcal{N}(s, l-1) \leq 2n(s, l-1) \leq \frac{2(l-s-1)}{T_D}$ , we obtain

$$\begin{aligned} \sum_{s=0}^{l-1} \sum_{h+r=s} \mu^{\mathcal{N}(s,l-1)} \alpha^{|\mathcal{F}_1(s,l-1)|} \beta^{-|\mathcal{F}_2(s,l-1)|} y^T(h,r) y(h,r) &< \sum_{s=0}^{l-1} \sum_{h+r=s} \varepsilon^{(l-1-s)} \vartheta^2 \omega^T(h,r) \omega(h,r) \\ &< \sum_{s=0}^{l-1} \sum_{h+r=s} \vartheta^2 \omega^T(h,r) \omega(h,r). \end{aligned}$$

Furthermore, it follows from  $\mu > 1$  and  $\beta > 1$  that

$$\sum_{s=0}^{l-1} \sum_{h+r=s} \left(\frac{1}{\beta}\right)^{(l-1-s)} y^T(h,r) y(h,r) < \sum_{s=0}^{l-1} \sum_{h+r=s} \vartheta^2 \omega^T(h,r) \omega(h,r). \quad (29)$$

Then, the following inequality can be deduced from (29):

$$\sum_{l=0}^{\infty} \sum_{s=0}^{l-1} \sum_{h+r=s} \left(\frac{1}{\beta}\right)^{(l-1-s)} y^T(h,r) y(h,r) < \sum_{l=0}^{\infty} \sum_{s=0}^{l-1} \sum_{h+r=s} \vartheta^2 \omega^T(h,r) \omega(h,r).$$

Note that from  $\sum_{l=s+1}^{\infty} \left(\frac{1}{\beta}\right)^{(l-1-s)} = 1 + \frac{1}{\beta} + \frac{1}{\beta^2} + \dots = \frac{\beta}{\beta-1} > 1$ , we derive

$$\sum_{s=0}^{\infty} \sum_{h+r=s} y^T(h,r) y(h,r) < \sum_{s=0}^{\infty} \sum_{h+r=s} \vartheta^2 \omega^T(h,r) \omega(h,r),$$

which means that Eq. (12) is satisfied. The proof is completed.

**Remark 4.** Notably, Theorem 1 provides sufficient criteria for the exponential stability and  $H_{\infty}$  DAP of the SMD in (10) under DoS-A. However, conditions (24) and (25) in Theorem 1 cannot be solved directly because of the existence of unknown gain matrices  $K_{\theta}$  and  $L_{\theta}$  in  $\tilde{A}_{\theta}$ . Consequently, solvable conditions will be further given in Subsection 3.2, which can be effectively solved by available software.

### 3.2 Sliding surface design

In this subsection, we investigate the existence of a sliding surface (6) and further provide the design method of the gain matrix in (6).

**Theorem 2.** Consider the 2D dynamic process in (1) under DoS-A satisfying Assumptions 1 and 2 with the scalars  $0 < \varepsilon < 1$ ,  $\vartheta > 0$ , and  $\alpha, \beta, \mu > 1$ . If the matrices  $X_{\theta} = \text{diag}\{X_{\theta 1}^1, X_{\theta 2}^1, X_{\theta 1}^2, X_{\theta 2}^2\} > 0$ ,  $\bar{K}_{1\theta}$ ,  $\bar{K}_{2\theta}$ ,  $\bar{L}_{1\theta}$ ,  $\bar{L}_{2\theta}$ ,  $Y$ ,  $R$ ,  $\bar{Y}$ , and  $\bar{R}$  exist, such that the following conditions:

$$C_1 X_{02}^1 = Y C_1, \quad C_2 X_{02}^2 = \bar{Y} C_2, \quad (30)$$

$$C_1 X_{11}^1 = R C_1, \quad C_2 X_{11}^2 = \bar{R} C_2, \quad (31)$$

$$\Psi_0 \triangleq [\Psi_0(h,r)]^{4 \times 4} < 0, \quad (32)$$

$$\Psi_1 \triangleq [\Psi_1(h,r)]^{4 \times 4} < 0, \quad (33)$$

hold with (14) and (15), where

$$\Psi_0(1,1) = \text{diag} \left\{ -\frac{1}{\beta} X_{01}^1, -\frac{1}{\beta} X_{02}^1, -\frac{1}{\beta} X_{01}^2, -\frac{1}{\beta} X_{02}^2 \right\}, \quad \Psi_0(1,3) = [\bar{\Psi}(h,r)]^{4 \times 4}, \quad \Psi_0(2,2) = -\vartheta^2 I,$$

$$\Psi_0(3,3) = \text{diag}\{-X_{01}^1, -X_{02}^1, -X_{01}^2, -X_{02}^2\}, \quad \Psi_0(4,4) = -I, \quad \Psi_1(1,3) = [\tilde{\Psi}(h,r)]^{4 \times 4},$$

$$\Psi_1(1,1) = \text{diag}\{-\alpha X_{11}^1, -\alpha X_{12}^1, -\alpha X_{11}^2, -\alpha X_{12}^2\}, \quad \Psi_1(2,2) = -\vartheta^2 I, \quad \Psi_1(4,4) = -I,$$

$$\Psi_1(3,3) = \text{diag}\{-X_{11}^1, -X_{12}^1, -X_{11}^2, -X_{12}^2\}, \quad \bar{G}_{10} = (G_{10} B_1 + G_{20} B_2)^{-1} G_{10},$$

$$\Psi_0(1,4) = \begin{bmatrix} X_{01}^1 C_1^T \\ X_{02}^1 C_1^T \\ X_{01}^2 C_2^T \\ X_{02}^2 C_2^T \end{bmatrix}, \quad \Psi_0(2,3)^T = \Psi_1(2,3)^T = \begin{bmatrix} 0 \\ 0 \\ D_1 \\ D_2 \end{bmatrix}, \quad \Psi_1(1,4) = \begin{bmatrix} X_{11}^1 C_1^T \\ X_{12}^1 C_1^T \\ X_{11}^2 C_2^T \\ X_{12}^2 C_2^T \end{bmatrix},$$

$$\begin{aligned} \bar{\Psi}(1,1) &= X_{01}^1 A_{11}^T + \bar{K}_{10}^T B_1^T, \quad \bar{\Psi}(1,2) = X_{01}^1 A_{21}^T + \bar{K}_{10}^T B_2^T, \quad \bar{G}_{20} = (G_{10} B_1 + G_{20} B_2)^{-1} G_{20}, \\ \bar{\Psi}(2,1) &= C_1^T \bar{L}_{10}^T - C_1^T \bar{L}_{10}^T \bar{G}_{10}^T B_1^T - C_1^T \bar{L}_{20}^T \bar{G}_{20}^T B_1^T, \quad \bar{\Psi}(2,3) = X_{02}^1 A_{11}^T - C_1^T \bar{L}_{10}^T, \\ \bar{\Psi}(2,2) &= C_1^T \bar{L}_{20}^T - C_1^T \bar{L}_{10}^T \bar{G}_{10}^T B_2^T - C_1^T \bar{L}_{20}^T \bar{G}_{20}^T B_2^T, \quad \bar{\Psi}(2,4) = X_{02}^1 A_{21}^T - C_1^T \bar{L}_{20}^T, \\ \bar{\Psi}(3,1) &= X_{01}^2 A_{12}^T + \bar{K}_{20}^T B_1^T, \quad \bar{\Psi}(3,2) = X_{01}^2 A_{22}^T + \bar{K}_{20}^T B_2^T, \quad \bar{G}_{11} = (G_{11} B_1 + G_{21} B_2)^{-1} G_{11}, \\ \bar{\Psi}(4,1) &= C_2^T \bar{L}_{10}^T - C_2^T \bar{L}_{10}^T \bar{G}_{10}^T B_1^T - C_2^T \bar{L}_{20}^T \bar{G}_{20}^T B_1^T, \quad \bar{\Psi}(4,3) = X_{02}^2 A_{12}^T - C_2^T \bar{L}_{10}^T, \\ \bar{\Psi}(4,2) &= C_2^T \bar{L}_{20}^T - C_2^T \bar{L}_{10}^T \bar{G}_{10}^T B_2^T - C_2^T \bar{L}_{20}^T \bar{G}_{20}^T B_2^T, \quad \bar{\Psi}(4,4) = X_{02}^2 A_{22}^T - C_2^T \bar{L}_{20}^T, \\ \tilde{\Psi}(1,1) &= X_{11}^1 A_{11}^T + \bar{K}_{11}^T B_1^T - C_1^T \bar{L}_{11}^T + C_1^T \bar{L}_{11}^T \bar{G}_{11}^T B_1^T + C_1^T \bar{L}_{21}^T \bar{G}_{21}^T B_1^T, \quad \tilde{\Psi}(1,3) = C_1^T \bar{L}_{11}^T, \\ \tilde{\Psi}(1,2) &= X_{11}^1 A_{21}^T + \bar{K}_{11}^T B_2^T - C_1^T \tilde{L}_{21}^T + C_1^T \bar{L}_{11}^T \bar{G}_{11}^T B_2^T + C_1^T \tilde{L}_{21}^T \bar{G}_{21}^T B_2^T, \quad \tilde{\Psi}(1,4) = C_1^T \tilde{L}_{21}^T, \\ \tilde{\Psi}(2,3) &= X_{12}^1 A_{11}^T, \quad \tilde{\Psi}(2,4) = X_{12}^1 A_{21}^T, \quad \bar{G}_{21} = (G_{11} B_1 + G_{21} B_2)^{-1} G_{21}, \\ \tilde{\Psi}(3,1) &= X_{11}^2 A_{12}^T + \bar{K}_{21}^T B_1^T - C_2^T \tilde{L}_{11}^T + C_2^T \tilde{L}_{11}^T \bar{G}_{11}^T B_1^T + C_2^T \bar{L}_{21}^T \bar{G}_{21}^T B_1^T, \\ \tilde{\Psi}(3,2) &= X_{11}^2 A_{22}^T + \bar{K}_{21}^T B_2^T - C_2^T \bar{L}_{21}^T + C_2^T \tilde{L}_{11}^T \bar{G}_{11}^T B_2^T + C_2^T \bar{L}_{21}^T \bar{G}_{21}^T B_2^T, \\ \tilde{\Psi}(3,3) &= C_2^T \tilde{L}_{11}^T, \quad \tilde{\Psi}(3,4) = C_2^T \bar{L}_{21}^T, \quad \tilde{\Psi}(4,3) = X_{12}^2 A_{12}^T, \quad \tilde{\Psi}(4,4) = X_{12}^2 A_{22}^T. \end{aligned}$$

Moreover, the gain matrices can be rewritten as follows:

$$K_{1\theta} = \bar{K}_{1\theta} (X_{\theta 1}^1)^{-1}, \quad K_{2\theta} = \bar{K}_{2\theta} (X_{\theta 1}^2)^{-1}, \quad L_{10} = \bar{L}_{10} Y^{-1}, \quad L_{20} = \bar{L}_{20} \bar{Y}^{-1}, \quad L_{11} = \bar{L}_{11} R^{-1}, \quad L_{21} = \bar{L}_{21} \bar{R}^{-1}. \quad (34)$$

Then, the SMD in (10) is ES with an  $H_\infty$  DAP  $\vartheta$ .

*Proof.* First, the objective is to verify that condition (32) is equivalent to (24). Let  $X_0 = P_0^{-1}$ . Pre-multiplying and post-multiplying condition (24) with  $\text{diag}\{X_0, I, \Xi^T X_0, I\}$  and  $\text{diag}\{X_0, I, X_0 \Xi, I\}$ , respectively, we obtain the following inequality:

$$\begin{bmatrix} -\frac{1}{\beta} X_0 & 0 & X_0 \Xi A_0^T & X_0 \Xi \bar{C}^T \\ * & -\vartheta^2 I & \bar{D}^T & 0 \\ * & * & -\Xi^T X_0 \Xi & 0 \\ * & * & * & -I \end{bmatrix} < 0. \quad (35)$$

Furthermore, substituting  $\bar{K}_{10} = K_{10} X_{01}^1$ ,  $\bar{K}_{20} = K_{20} X_{01}^2$ ,  $\bar{L}_{10} = L_{10} Y$ ,  $\bar{L}_{20} = L_{20} \bar{Y}$ ,  $\tilde{L}_{10} = \bar{L}_{10} Y^{-1} \bar{Y}$ , and  $\bar{L}_{20} = \bar{L}_{20} \bar{Y}^{-1} \bar{Y}$  into (35) yields (32).

Similarly, using  $\text{diag}\{X_1, I, \Xi^T X_1, I\}$  and  $\text{diag}\{X_1, I, X_1 \Xi, I\}$  to pre-multiply and post-multiply (25) and letting  $X_1 = P_1^{-1}$ ,  $\bar{K}_{11} = K_{11} X_{11}^1$ ,  $\bar{K}_{21} = K_{21} X_{11}^2$ ,  $\bar{L}_{11} = L_{11} R$ ,  $\bar{L}_{21} = L_{21} \bar{R}$ ,  $\tilde{L}_{11} = \bar{L}_{11} R^{-1} \bar{R}$ , and  $\bar{L}_{21} = \bar{L}_{21} \bar{R}^{-1} \bar{R}$ , we can obtain (33). This completes the proof.

**Remark 5.** According to Theorem 2, the gains of the estimator and sliding mode controller can be obtained by solving the LMIs (14), (15), (32), and (33) using the linear matrix equality (LME) in (30) and (31). Nevertheless, solving the LME using the LMI toolbox of MATLAB is rather difficult. Therefore, using the method proposed in [44], condition (31) can be replaced by the following inequalities:

$$\begin{bmatrix} -\lambda I & * \\ C_1 X_{02}^1 - Y C_1 & -I \end{bmatrix} < 0, \quad \begin{bmatrix} -\lambda I & * \\ C_2 X_{02}^2 - \bar{Y} C_2 & -I \end{bmatrix} < 0, \quad (36)$$

$$\begin{bmatrix} -\lambda I & * \\ C_1 X_{11}^1 - R C_1 & -I \end{bmatrix} < 0, \quad \begin{bmatrix} -\lambda I & * \\ C_2 X_{11}^2 - \bar{R} C_2 & -I \end{bmatrix} < 0, \quad (37)$$

where  $\lambda$  is a given sufficiently small positive constant. Then, the gain matrices can be solved by determining the solution to the following convex optimization problem:

$$\min \vartheta \quad \text{subject to (15), (16), (34), (35), (38), and (39)}. \quad (38)$$

---

**Algorithm 1** Design algorithm of resilient SMC for 2DSs
 

---

```

1: Given system parameter matrices  $A, B, C, D$  in (1) and matrix  $G_\theta$  in (6);
2: Set up the corresponding parameters  $\varepsilon, \alpha, \beta, \mu, \lambda, \Lambda, T_A$ , and  $T_D$ ;
3: if Eq. (15) is unsatisfied then
4:   Return to Step 2;
5: else
6:   Set the upper threshold of the time interval  $T_u$ ;
7:   Generate the DoS-A based on Assumptions 1 and 2;
8: end if
9: if a feasible solution to (38) can be obtained, then
10:  Calculate the estimator and controller gain matrices  $L_\theta$  and  $K_\theta$  in (5) and (6);
11:  for  $h = 1 : T_u$  do
12:    for  $r = 1 : T_u$  do
13:      Verify the system performance and compute the sliding variable and SMC scheme;
14:    end for
15:  end for
16: else
17:   Output "The convex optimization problem (38) has on solution";
18:   Return to Step 1;
19: end if
    
```

---

### 3.3 Resilient sliding mode controller design

In this subsection, we focus on the design of the resilient SMC scheme.

**Theorem 3.** Consider the 2D dynamic process in (1) under DoS-A satisfying Assumptions 1 and 2. Then, the state trajectories of the SMD (10) can be forced into a neighborhood of the proposed sliding surface  $s(h, r) = 0$  in (6) and remain in it using the following controller:

$$u(h, r) = K_\theta \hat{x}(h, r) - (G_\theta B)^{-1} \|G_\theta L_\theta e_y(h, r)\| \text{sign}(s(h, r)) - (G_\theta B)^{-1} \Lambda s(h, r), \quad (39)$$

where  $\Lambda > 0$  is the adjusting matrix.

*Proof.* For the analysis of reachability, if the following Lyapunov candidate is chosen:

$$V(s(h, r)) = \frac{1}{2} s^T(h, r) s(h, r), \quad (40)$$

then the incremental  $\Delta V(s(h, r))$  is  $\Delta V(s(h, r)) = V(\bar{s}(h, r)) - V(s(h, r))$  with  $\bar{s}(h, r) = \begin{bmatrix} s^1(h+1, r) \\ s^2(h, r+1) \end{bmatrix}$ . By combining (6) and (7) with  $\Delta s(h, r) = \bar{s}(h, r) - s(h, r)$ , we obtain

$$\begin{aligned} \Delta V(s(h, r)) &= \frac{1}{2} \bar{s}^T(h, r) \bar{s}(h, r) - \frac{1}{2} s^T(h, r) s(h, r) = \frac{1}{2} [(\bar{s}^T(h, r) + s^T(h, r))(\bar{s}(h, r) - s(h, r))] \\ &= \frac{1}{2} [2s^T(h, r) + \Delta s(h, r)] \Delta s(h, r) = s^T(h, r) [\bar{s}(h, r) - s(h, r)] + \frac{1}{2} \Delta s^T(h, r) \Delta s(h, r) \\ &= s^T(h, r) [G_\theta B u(h, r) + G_\theta L_\theta e_y(h, r) - G_\theta B K_\theta \hat{x}(h, r) - s(h, r)] + \frac{1}{2} \Delta s^T(h, r) \Delta s(h, r). \end{aligned} \quad (41)$$

Furthermore, substituting (39) into (41) yields  $\Delta V(s(h, r)) \leq -s^T(h, r)(I + \Lambda)s(h, r) + \frac{1}{2} \Delta s^T(h, r) \Delta s(h, r)$ . A suitable and sufficiently large  $\Lambda$  matrix can be chosen such that  $\Delta V(s(h, r)) < 0$  when  $s(h, r)$  is outside a certain bounded region. Notably, although  $\Delta s(h, r)$  does not asymptotically tend to zero, it is reasonably bounded. Therefore, the trajectory of (10) can be driven to a region near the sliding mode surface by the control law (39) and remains in it thereafter. The proof is completed.

**Remark 6.** The main steps of SMC design (i.e., sliding surface and SMC law design) have been accomplished, as indicated by the previously presented results. In Theorem 2, sufficient conditions have been proposed such that the SMD in (10) exhibits exponential stability and desirable  $H_\infty$  performance. Moreover, in Theorem 3, a resilient sliding mode controller has been developed for 2D dynamics under DoS-A to enforce the trajectories of the system (10) to the designed sliding surface and maintain it all the time. Compared with the existing research on the SMC problem of 2DSs, the issue of resilient SMC for 2D dynamic processes in the presence of DoS-A is investigated in our work, which is the first to address the resilient SMC problem of 2DSs under DoS-A.

Furthermore, the design algorithm of resilient SMC for 2DSs is summarized in Algorithm 1.

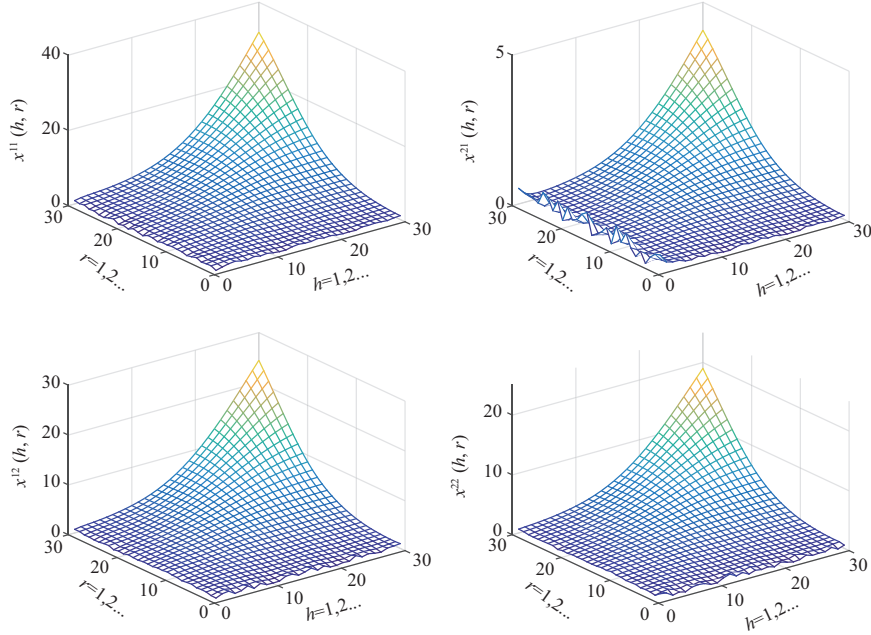


**Figure 3** (Color online) State responses of the open-loop system.

## 4 Illustrative example

In this section, we verify the effectiveness of the presented resilient SMC scheme using the following examples.

**Example 1.** Consider the 2D dynamic process (1) with

$$\begin{aligned}
 A_{11} &= \begin{bmatrix} 0.5 & 0.5 \\ 0.01 & 0.4 \end{bmatrix}, \quad A_{12} = \begin{bmatrix} 0.6 & 0.1 \\ 0.1 & 0 \end{bmatrix}, \quad A_{21} = \begin{bmatrix} 0.45 & 0.20 \\ 0.25 & 0.30 \end{bmatrix}, \quad A_{22} = \begin{bmatrix} 0.40 & 0.05 \\ 0.45 & 0 \end{bmatrix}, \\
 B_1 &= \begin{bmatrix} 0.1 \\ 0.1 \end{bmatrix}, \quad B_2 = \begin{bmatrix} 0.1 \\ 0.1 \end{bmatrix}, \quad C_1 = [0.03 \ 0], \quad C_2 = [0.01 \ -0.01], \quad D_1 = \begin{bmatrix} 0.01 \\ -0.02 \end{bmatrix}, \\
 D_2 &= \begin{bmatrix} 0.02 \\ 0.04 \end{bmatrix}, \quad G_{10} = [0.2 \ 0.1], \quad G_{20} = [0.1 \ 0.2], \quad G_{11} = [0.12 \ -0.1], \quad G_{21} = [-0.1 \ 0].
 \end{aligned}$$

First, the states of the corresponding open-loop case with the aforementioned parameters are shown in Figure 3.

In (3) and (4), the parameters of DoS-A are set as  $T_D = 10$  and  $T_A = 8$ . In addition, the scalars in Theorem 2 are set as  $\varepsilon = 0.4$ ,  $\alpha = 1.2$ ,  $\beta = 5.6$ ,  $\mu = 3$ ,  $\lambda = 0.0001$ , and  $\Lambda = 0.2$ . Then, we obtain  $\frac{\ln(\mu)}{\ln(\varepsilon)+\ln(\beta)} = 1.3622 < \frac{T_D}{3}$ ,  $\frac{\ln(\alpha)+\ln(\beta)}{\ln(\varepsilon)+\ln(\beta)} = 2.3622 < \frac{T_A}{3}$ , and  $\ln(\varepsilon) + \ln(\beta) = 0.8065 > 0$ . The corresponding DoS-A is depicted in Figure 4, where the transmissions are secure as  $\theta = 0$ , and the attacks occur as  $\theta = 1$ .

Furthermore, from Theorem 2, the estimator and controller gain matrices can be designed as follows:

$$\begin{aligned}
 L_0^T &= [13.1134 \ 0.3776 \ 16.0287 \ 20.8417], \quad L_1^T = [8.3448 \ -5.5255 \ -0.6877 \ 0.2456], \\
 K_0 &= [-4.0982 \ -2.4546 \ -4.7248 \ -0.9130], \quad K_1 = [-1.0663 \ -4.5505 \ -2.8364 \ -0.9945]
 \end{aligned}$$

with the optimal  $H_\infty$  performance index  $\vartheta^* = 0.1936$ . Meanwhile, when the system works in a secure network environment, the corresponding performance index  $\vartheta^* = 0.1229$ . Notably, the system performance is degraded under DoS-A.

Then, the BC is set as

$$x^1(1, r) = x^2(r, 1) = \begin{cases} [\text{rand}(1) \ \text{rand}(1)]^T, & 1 \leq r \leq 30, \\ [0 \ 0]^T, & r > 30. \end{cases}$$

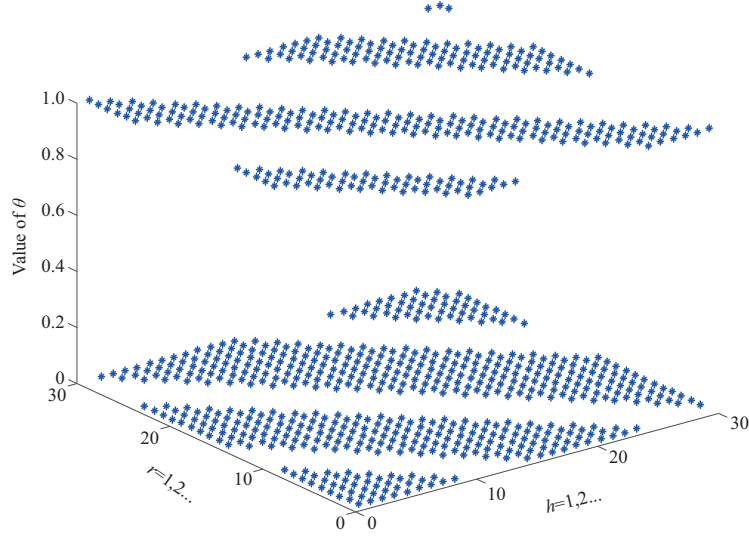


Figure 4 (Color online) Switching mechanism under DoS-A.

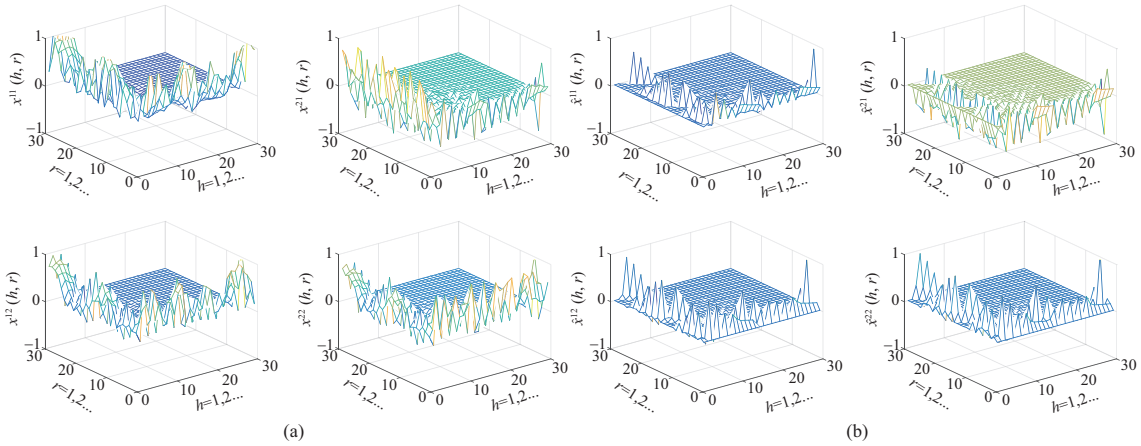


Figure 5 (Color online) (a) Trajectories and (b) estimation of the system state.

The external disturbance  $\omega(h, r)$  is assumed to be white noise with  $\mathbb{E}\{\omega(h, r)\} = 0$  and  $\mathbb{D}\{\omega(h, r)\} = 1$  when  $0 \leq h, r \leq 15$ , and  $\omega(h, r) = 0.1$  when  $h, r > 15$ . The simulation results are shown in Figures 5(a) and (b). Figure 5(a) plots the state responses of the system. Figure 5(b) depicts the estimation of the system state. Moreover, Figures 6(a) and (b) show the evolution of the sliding variable  $s(h, r)$  and SMC scheme  $u(h, r)$ , respectively. Figures 6(a) and (b) illustrate that the proposed control scheme is indeed effective. In addition,  $\vartheta^* > \bar{\vartheta}^*$  indicates that attack resilience is achieved at the cost of  $H_\infty$  performance to some extent.

**Example 2.** In real-world applications, many dynamic procedures, such as infectious disease forecasting [45], fluid motion [46], and investment securities [47], can be depicted by the Darboux-type equation:

$$\frac{\partial^2 s(x, t)}{\partial x \partial t} = a_0 s(x, t) + a_1 \frac{\partial s(x, t)}{\partial t} + a_2 \frac{\partial s(x, t)}{\partial x} + b_1 u(x, t) + b_0 \omega(h, r). \quad (42)$$

Furthermore, inspired by the method employed in [48], the model in (42) can be transformed into a 2D Roesser model with

$$A = \begin{bmatrix} 1 + a_1 \Delta x & (a_0 + a_1 a_2) \Delta x \\ \Delta t & 1 + a_2 \Delta t \end{bmatrix}, \quad B = \begin{bmatrix} b_1 \Delta x \\ 0 \end{bmatrix}, \quad D = \begin{bmatrix} b_0 \Delta x \\ 0 \end{bmatrix}.$$

With the choice of coefficients  $a_0 = 2, a_1 = 0.1, a_2 = -2, b_1 = 1, b_0 = 1, \Delta x = 0.1$ , and  $\Delta t = 0.2$ , the

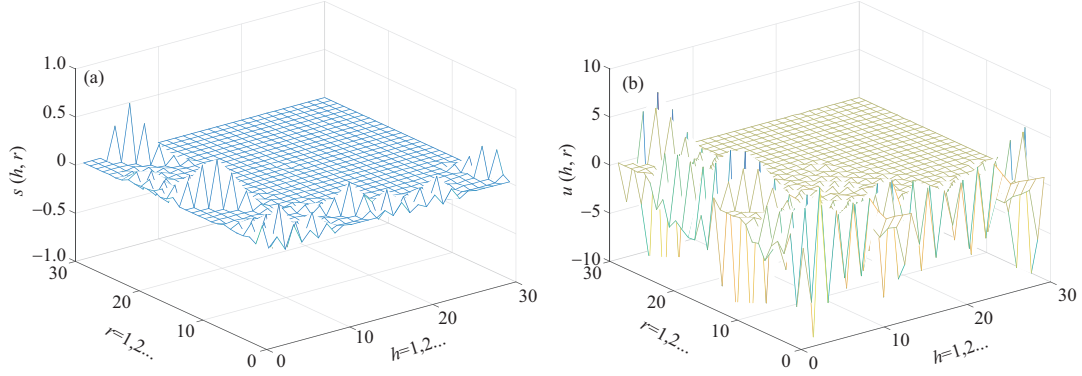


**Figure 6** (Color online) (a) Sliding mode surface function  $s(h, r)$  and (b) sliding mode controller  $u(h, r)$ .

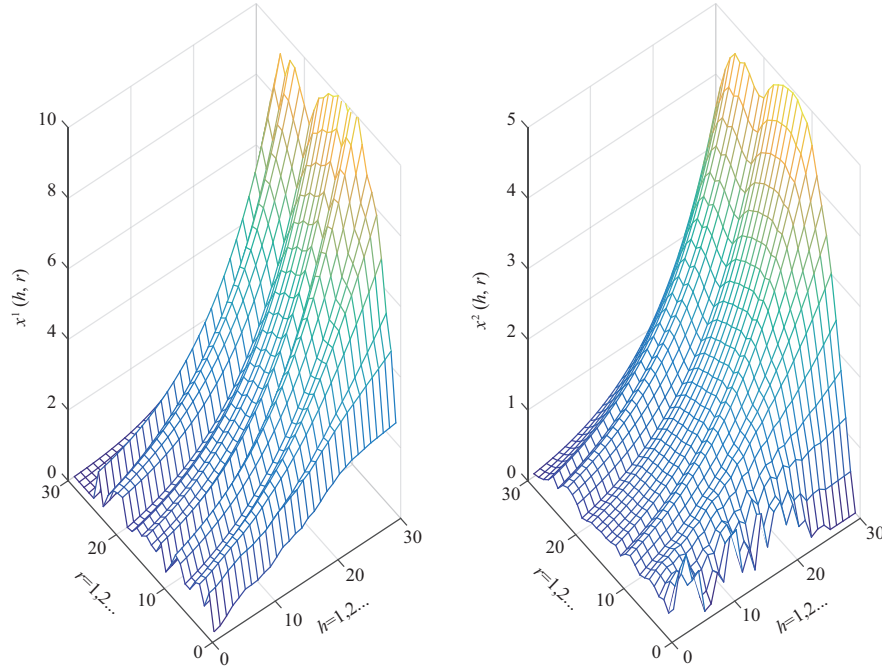


**Figure 7** (Color online) State responses of the open-loop system.

system matrices of formula (1) are obtained as follows:

$$A = \begin{bmatrix} 1.01 & 0.18 \\ 0.2 & 0.6 \end{bmatrix}, B = \begin{bmatrix} 0.1 \\ 0 \end{bmatrix}, D = \begin{bmatrix} 0.1 \\ 0 \end{bmatrix}.$$

Other matrices are designated as  $C = [0.03 \ 0.01]$ ,  $G_0 = [0.2 \ 0.1]$ , and  $G_1 = [0.12 \ -0.1]$ . Figure 7 illustrates the state responses of the open-loop case.

Similarly, by setting  $T_D = 10$  and  $T_A = 8$  and choosing the parameters  $\alpha = 1.2, \beta = 2.7, \mu = 3, \lambda = 0.0001, \varepsilon = 0.6$ , and  $\Lambda = 0.2$ , condition (15) is satisfied. The initial condition is set as

$$x^1(1, r) = x^2(r, 1) = \begin{cases} \text{rand}(1), & 1 \leq r \leq 25, \\ 5e^{-r}, & 25 < r \leq 30, \\ 0, & r > 30, \end{cases}$$

and  $\omega(h, r)$  remains the same as the external disturbance in Example 1.

From Theorem 2, we obtain the  $H_\infty$  performance index  $\vartheta^* = 0.2663$ . Furthermore, the parameters of

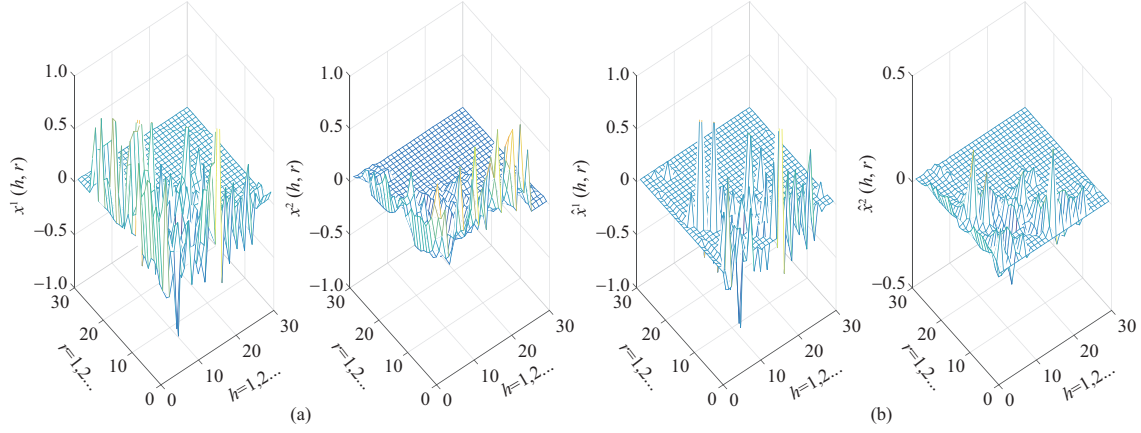


**Figure 8** (Color online) (a) Trajectories and (b) estimation of the system state.

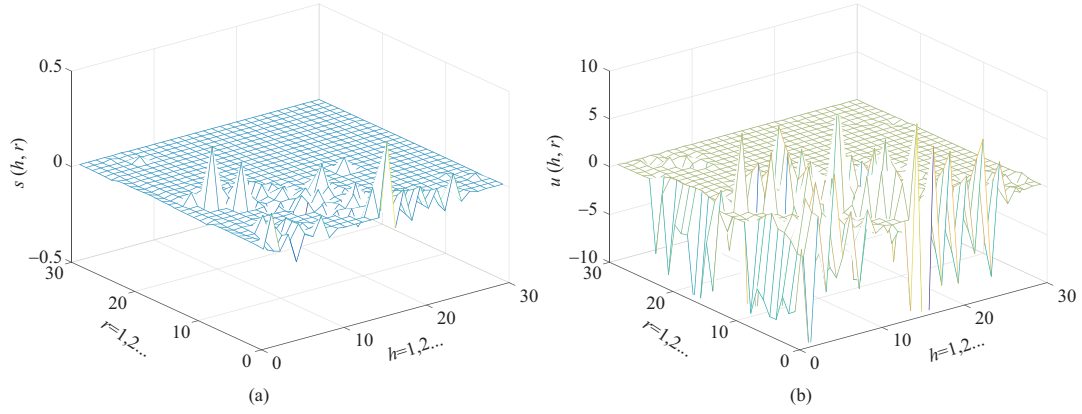


**Figure 9** (Color online) (a) Sliding mode surface function  $s(h, r)$  and (b) sliding mode controller  $u(h, r)$ .

the estimator and controller corresponding to the case of  $\vartheta^* = 0.2663$  are calculated as follows:

$$L_0 = \begin{bmatrix} 33.6667 \\ 1.5004 \end{bmatrix}, L_1 = \begin{bmatrix} -1.6485 \\ 5.0730 \end{bmatrix}, K_0 = \begin{bmatrix} -10.0243 & -1.7739 \end{bmatrix}, K_1 = \begin{bmatrix} -9.9810 & -1.3772 \end{bmatrix}.$$

Notably, the optimal  $H_\infty$  performance index is  $\vartheta^* = 0.0443$  for a secure network environment. Moreover, the verification results are presented in Figures 8(a) and (b), which show the system state and its estimation, respectively. Figures 9(a) and (b) depict the sliding variable and SMC scheme, respectively. These results show the effectiveness of the proposed method.

## 5 Conclusion

In this study, the resilient SMC issue of 2D CPSs encountering DoS-A has been solved. The PL of CPSs has been described as a 2D Roesser model, and the sensor attack has been discussed. Given that malicious attacks are not always persistent, the relevant assumptions have been given on the average frequency and duration of DoS-A. Furthermore, given the DoS-A situation, the underlying system has been represented as a switched system. Then, by combining the Lyapunov theory of switched systems and the LMI approach, sufficient criteria have been provided to ensure that the SMD is ES with an  $H_\infty$  DAP. Based on the previously obtained results, the resilient SMC law has been established, and the reachability of the SMD has been analyzed. Finally, the proposed SMC scheme has been validated using two examples. Future work will include an extension to the problems of security state estimation and defense-based resilient control for 2D CPSs under malicious attacks.

**Acknowledgements** This work was supported in part by National Natural Science Foundation of China (Grant Nos. 62273208, 62033005, 62320106001, 62103118, 62373127), Natural Science Foundation of Heilongjiang Province (Grant No. ZD2021F001),

Science Center Program of National Natural Science Foundation of China (Grant No. 62188101), Heilongjiang Touyan Team Program, and China Postdoctoral Science Foundation (Grant Nos. 2021T140160, 2021M700037).

## References

- 1 Lu A Y, Yang G H. Observer-based control for cyber-physical systems under denial-of-service with a decentralized event-triggered scheme. *IEEE Trans Cybern*, 2020, 50: 4886–4895
- 2 Li Y, Quevedo D E, Dey S, et al. SINR-based DoS attack on remote state estimation: a game-theoretic approach. *IEEE Trans Control Netw Syst*, 2017, 4: 632–642
- 3 Sun Y C, Yang G H. Event-triggered remote state estimation for cyber-physical systems under malicious DoS attacks. *Inf Sci*, 2022, 602: 43–56
- 4 Chen H, Zong G, Zhao X, et al. Secure filter design of fuzzy switched CPSs with mismatched modes and application: a multidomain event-triggered strategy. *IEEE Trans Ind Inf*, 2023, 19: 10034–10044
- 5 Chen H, Zong G, Gao F, et al. Probabilistic event-triggered policy for extended dissipative finite-time control of MJSs under cyber-attacks and actuator failures. *IEEE Trans Automat Contr*, 2023, 68: 7803–7810
- 6 Yang D, Zong G, Shi Y, et al. Adaptive tracking control of hybrid switching markovian systems with its applications. *SIAM J Control Optim*, 2023, 61: 434–457
- 7 Fawzi H, Tabuada P, Diggavi S. Secure estimation and control for cyber-physical systems under adversarial attacks. *IEEE Trans Automat Contr*, 2014, 59: 1454–1467
- 8 Wu C, Hu Z, Liu J, et al. Secure estimation for cyber-physical systems via sliding mode. *IEEE Trans Cybern*, 2018, 48: 3420–3431
- 9 Jin X, Haddad W M, Yucelen T. An adaptive control architecture for mitigating sensor and actuator attacks in cyber-physical systems. *IEEE Trans Automat Contr*, 2017, 62: 6058–6064
- 10 de Persis C, Tesi P. Input-to-state stabilizing control under denial-of-service. *IEEE Trans Automat Contr*, 2015, 60: 2930–2944
- 11 Feng S, Tesi P. Resilient control under denial-of-service: robust design. *Automatica*, 2017, 79: 42–51
- 12 Wu C, Wu L, Liu J, et al. Active defense-based resilient sliding mode control under denial-of-service attacks. *IEEE Trans Inform Forensic Secur*, 2019, 15: 237–249
- 13 Befekadu G K, Gupta V, Antsaklis P J. Risk-sensitive control under Markov modulated denial-of-service (DoS) attack strategies. *IEEE Trans Automat Contr*, 2015, 60: 3299–3304
- 14 Ma R, Shi P, Wu L. Dissipativity-based sliding-mode control of cyber-physical systems under denial-of-service attacks. *IEEE Trans Cybern*, 2021, 51: 2306–2318
- 15 Zhu Y, Zheng W X. Observer-based control for cyber-physical systems with periodic DoS attacks via a cyclic switching strategy. *IEEE Trans Automat Contr*, 2019, 65: 3714–3721
- 16 Hu S, Yue D, Xie X, et al. Resilient event-triggered controller synthesis of networked control systems under periodic DoS jamming attacks. *IEEE Trans Cybern*, 2019, 49: 4271–4281
- 17 Dolk V S, Tesi P, Persis C D, et al. Event-triggered control systems under denial-of-service attacks. *IEEE Trans Control Netw Syst*, 2017, 4: 93–105
- 18 Tian Y X, Li X, Dong B, et al. Event-based sliding mode control under denial-of-service attacks. *Sci China Inf Sci*, 2022, 65: 162203
- 19 Liu D R. Lyapunov stability of two-dimensional digital filters with overflow nonlinearities. *IEEE Trans Circuits Syst I*, 1998, 45: 574–577
- 20 Bose N K. *Multidimensional Systems Theory and Applications*. Dordrecht: Kluwer, 2003
- 21 Lu W S, Antoniou A. *Two-Dimensional Digital Filters*. New York: Marcel Dekker, 1992
- 22 de Souza C E, Xie L, Coutinho D F. Robust filtering for 2-D discrete-time linear systems with convex-bounded parameter uncertainty. *Automatica*, 2010, 46: 673–681
- 23 Ahn C K, Shi P, Basin M V. Two-dimensional dissipative control and filtering for Roesser model. *IEEE Trans Automat Contr*, 2015, 60: 1745–1759
- 24 Wu L, Yang R, Shi P, et al. Stability analysis and stabilization of 2-D switched systems under arbitrary and restricted switchings. *Automatica*, 2015, 59: 206–215
- 25 Wang Y, Zhao D, Li Y, et al. Unbiased minimum variance fault and state estimation for linear discrete time-varying two-dimensional systems. *IEEE Trans Automat Contr*, 2017, 62: 5463–5469
- 26 Wu L, Wang Z. *Filtering and Control for Classes of Two-Dimensional Systems*. London: Springer, 2015
- 27 Wu Z G, Shen Y, Shi P, et al.  $\mathcal{H}_\infty$  control for 2D Markov jump systems in Roesser model. *IEEE Trans Automat Contr*, 2019, 64: 427–432
- 28 Tao Y Y, Wu Z G, Guo Y. Two-dimensional asynchronous sliding-mode control of Markov jump Roesser systems. *IEEE Trans Cybern*, 2022, 52: 2543–2552
- 29 Yang R, Li L, Shi P. Dissipativity-based two-dimensional control and filtering for a class of switched systems. *IEEE Trans Syst Man Cybern Syst*, 2021, 51: 2737–2750
- 30 Liang J, Wang F, Wang Z, et al. Minimum-variance recursive filtering for two-dimensional systems with degraded measurements: boundedness and monotonicity. *IEEE Trans Automat Contr*, 2019, 64: 4153–4166
- 31 Zhu K, Wang Z, Dong H, et al. Set-membership filtering for two-dimensional systems with dynamic event-triggered mechanism. *Automatica*, 2022, 143: 110416
- 32 Ma R, Shi P, Wu L. Active resilient control for two-dimensional systems under denial-of-service attacks. *Intl J Robust Nonlinear*, 2021, 31: 759–771
- 33 Wang F, Wang Z, Liang J, et al. A recursive algorithm for secure filtering for two-dimensional state-saturated systems under network-based deception attacks. *IEEE Trans Netw Sci Eng*, 2022, 9: 678–688
- 34 Luo Y, Wang Z, Hu J, et al. Security-guaranteed fuzzy networked state estimation for 2-D systems with multiple sensor arrays subject to deception attacks. *IEEE Trans Fuzzy Syst*, 2023, 31: 3624–3638
- 35 Wu L, Zheng W X, Gao H. Dissipativity-based sliding mode control of switched stochastic systems. *IEEE Trans Automat Contr*, 2013, 58: 785–791
- 36 Liu J, Wu L, Wu C, et al. Event-triggering dissipative control of switched stochastic systems via sliding mode. *Automatica*, 2019, 103: 261–273
- 37 Cao Z, Niu Y, Song J. Finite-time sliding-mode control of Markovian jump cyber-physical systems against randomly occurring injection attacks. *IEEE Trans Automat Contr*, 2020, 65: 1264–1271

- 38 Song J, Wang Z, Niu Y. On  $H_\infty$  sliding mode control under stochastic communication protocol. *IEEE Trans Automat Contr*, 2019, 64: 2174–2181
- 39 Behera A K, Bandyopadhyay B, Yu X. Periodic event-triggered sliding mode control. *Automatica*, 2018, 96: 61–72
- 40 Yang R, Zheng W X, Yu Y. Event-triggered sliding mode control of discrete-time two-dimensional systems in Roesser model. *Automatica*, 2020, 114: 108813
- 41 Song J, Niu Y. Co-design of 2-D event generator and sliding mode controller for 2-D Roesser model via genetic algorithm. *IEEE Trans Cybern*, 2021, 51: 4581–4590
- 42 Yang R, Zheng W X. Model transformation based sliding mode control of discrete-time two-dimensional Fornasin-Marchesini systems. *J Franklin Inst*, 2019, 356: 2463–2473
- 43 Lv X, Niu Y, Song J. Sliding mode control for uncertain 2D systems under stochastic communication protocol: the Roesser model case. *IEEE Trans Circuits Syst II*, 2022, 69: 1228–1232
- 44 Zhang Y, Shi P, Nguang S K, et al. Observer-based finite-time fuzzy  $H_\infty$  control for discrete-time systems with stochastic jumps and time-delays. *Signal Processing*, 2014, 97: 252–261
- 45 Lee T S, Chen I F, Chang T J, et al. Forecasting weekly influenza outpatient visits using a two-dimensional hierarchical decision tree scheme. *Int J Environ Res Public Health*, 2020, 17: 4743
- 46 Soulis J V. Computation of two-dimensional dam-break flood flows. *Numer Methods Fluids*, 1992, 14: 631–664
- 47 Li X, Sun Y. Stock intelligent investment strategy based on support vector machine parameter optimization algorithm. *Neural Comput Applic*, 2020, 32: 1765–1775
- 48 van Hien L, Trinh H, Lan-Huong N T. Delay-dependent energy-to-peak stability of 2-D time-delay Roesser systems with multiplicative stochastic noises. *IEEE Trans Automat Contr*, 2019, 64: 5066–5073